Pis'ma v ZhETF, vol. 80, iss. 12, pp. 845 – 849

Systematization of tensor mesons and the determination of the 2^{++} glueball

V. V. Anisovich[1)]

St.-Petersburg Nuclear Physics Institute, 188300 Gatchina, Russia

Submitted 22 November 2004

It is shown that new data on the ($J^{PC} = 2^{++}$)-resonances in the mass range $M \sim 1700 - 2400$ MeV support the linearity of the (n, M^2)-trajectories, where n is the radial quantum number of quark–antiquark state. In this way all vacancies for the isoscalar tensor $q\bar{q}$-mesons in the range up to 2450 MeV are filled in. This allows one to fix the broad f_2-state with $M = 2000 \pm 30$ MeV and $\Gamma = 530 \pm 40$ MeV as the lowest tensor glueball.

PACS: 12.38.–t, 12.39.Mk, 14.40.–n

Recent phase space analysis of the process $\gamma\gamma \to \to K_S K_S$ [1] and re-analysis of $\phi\phi$-spectra [2] observed in the reaction $\pi^- p \to \phi\phi n$ [3] have clarified the situation with f_2-mesons in the mass region $1700 - 2400$ MeV. Hence, now one may definitely speak about the location of $q\bar{q}$-states on the (n, M^2)-trajectories [4], see also [5, 6]. This fact enables us to determine which one of f_2-mesons is an extra state for the (n, M^2)-trajectories. Such an extra state is the broad resonance $f_2(2000 \pm 30)$. According to [2, 7, 8], its parameters are as follows:

$$M = 2050 \pm 30 \text{ MeV}, \quad \Gamma = 570 \pm 70 \text{ MeV [2]},$$
$$M = 1980 \pm 20 \text{ MeV}, \quad \Gamma = 520 \pm 50 \text{ MeV [7]},$$
$$M = 2010 \pm 25 \text{ MeV}, \quad \Gamma = 495 \pm 35 \text{ MeV [8]}. \quad (1)$$

In [4], we have put quark–antiquark meson states with different radial excitations ($n = 1, 2, 3, 4, \ldots$) on the (n, M^2)-trajectories. With a good accuracy, the trajectories occurred to be linear:

$$M^2 \ = \ M_0^2 + (n-1)\mu^2 \ , \quad (2)$$

with a universal slope $\mu^2 = 1.2 \pm 0.1\,\text{GeV}^2$; M_0 is the mass of the lowest (basic) state. For the ($I = 0, J^{PC} = = 2^{++}$)-mesons, the present status of trajectories (i.e. with the results given by [1, 2]) are shown in Figure.

The quark states with ($I = 0, J^{PC} = 2^{++}$) are defined by two flavour components, $n\bar{n} = (u\bar{u} + d\bar{d})/\sqrt{2}$ and $s\bar{s}$, with ${}^{2S+1}L_J = {}^3P_2, {}^3F_2$. Generally, all mesons are the mixture of flavour component in the P- and F-waves. But, as concern the f_2-mesons with $M \lesssim 2$ GeV, they are dominated by the flavour component $n\bar{n}$ or $s\bar{s}$ in a definite P or F wave. The f_2-mesons shown in Figure, which belong to four trajectories, are dominated by the following states:

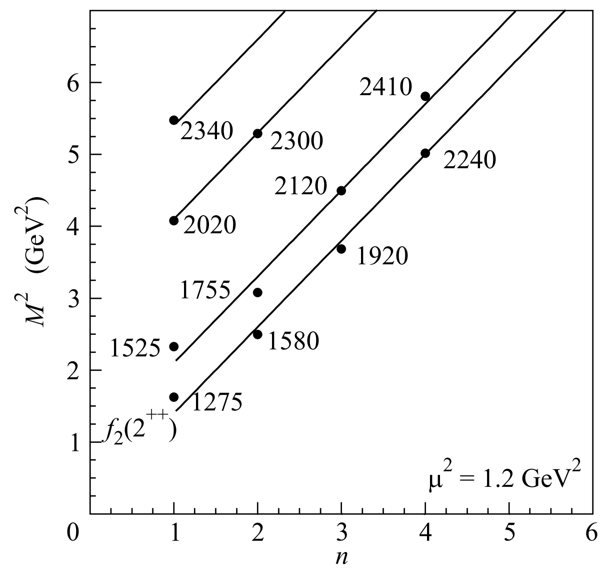

The f_2 trajectories of on the (n, M^2) plane; n is radial quantum number of $q\bar{q}$ state. The numbers stand for the experimentally observed f_2-meson masses M

$$\Big[f_2(1275), f_2(1580), f_2(1920), f_2(2240)\Big] \longrightarrow {}^3P_2 n\bar{n}\ ,$$
$$\Big[f_2(1525), f_2(1755), f_2(2120), f_2(2410)\Big] \longrightarrow {}^3P_2 s\bar{s}\ ,$$
$$\Big[f_2(2020),\ f_2(2300)\Big] \longrightarrow {}^3F_2 n\bar{n}\ ,$$
$$f_2(2340) \longrightarrow {}^3F_2 s\bar{s}\ . \quad (3)$$

To avoid the confusion, in (3) the experimentally observed masses of mesons are shown – these are the magnitudes drawn in Figure but not those from the compilation [9].

Let us discuss the states which lie on the trajectories of Figure.

1)e-mail: anisovic@pnpi.spb.ru

The trajectory [f_2(1275), f_2(1580), f_2(1920), f_2(2240)]. 1) $f_2(1275)$: This resonance is almost pure $1^3P_2n\bar{n}$-state: this is favoured by the comparison of branching ratios $f_2(1275) \to \pi\pi, \eta\eta, K\bar{K}$ with quark model calculations. The dominance of $1^3P_2n\bar{n}$ component is also supported by the value of partial width of the decay $f_2(1275) \to \gamma\gamma$ [10, 11].

2) $f_2(1580)$ (in the compilation [9] it is denoted as $f_2(1565)$): About ten years ago, there existed a number of indications to the presence of the 2^{++}-mesons in the vicinity of 1500 MeV [12–15]. After the discovery of a strong signal in the 0^{++}-wave related to the $f_0(1500)$ [16, 17] as well as correct account for the interference of 0^{++} and 2^{++} waves, the resonance signal in the 2^{++} wave moved towards higher masses, ~ 1570 MeV. According to the latest combined analysis of meson spectra [6, 18], this resonance has the following characteristics (see Table 1 in [6]):

$$M = 1580 \pm 6 \text{ MeV}, \quad \Gamma = 160 \pm 20 \text{ MeV}. \qquad (4)$$

Hadronic decays together with partial width in the channel $\gamma\gamma$ [10] support the $f_2(1580)$ as a system with dominant $n\bar{n}$-component.

In [9], the $f_2(1640)$-state is marked as a separate resonance: this identification is based on resonance signals at $M = 1620 \pm 16$ MeV [19] (Mark 3 data for $J/\Psi \to \gamma\pi^+\pi^-\pi^+\pi^-$), $M = 1647 \pm 7$ MeV [13] (reaction $\bar{n}p \to 3\pi^+2\pi^-$), $M = 1590 \pm 30$ MeV [20], 1635 ± 7 MeV [21] (reaction $\pi^-p \to \omega\omega n$). Without doubt, these signals are the reflections of $f_2(1580 \pm 20)$, and the data [19, 20] do not contradict this fact. In [9], the mass of this state is determined as 1638 ± 6 MeV that reflects small errors in the mass definition in [13, 21].

3) $f_2(1920)$ (in the compilation [9], it is denoted as $f_2(1910)$): This resonance was observed in the signals $\omega\omega$ [20–22] and $\eta\eta'$ [23, 24]. In [8], the $f_2(1920)$ is seen as a shoulder in the $p\bar{p}(I = 0, C = +1) \to \pi^0\pi^0, \eta\eta, \eta\eta'$ spectra, in the wave $^3P_2p\bar{p}$. According to [6, 18],

$$M = 1920 \pm 40 \text{ MeV}, \quad \Gamma = 260 \pm 40 \text{ MeV}. \qquad (5)$$

A strong signal in the channels with nonstrange mesons surmises a large $n\bar{n}$ component in the $f_2(1920)$.

4) $f_2(2240)$: It is seen in the spectra $p\bar{p}(I = 0, C = +1) \to \pi^0\pi^0, \eta\eta, \eta\eta'$, in the wave $^3P_2p\bar{p}$ [8]. According to [6, 18]:

$$M = 2240 \pm 30 \text{ MeV}, \quad \Gamma = 245 \pm 45 \text{ MeV}. \qquad (6)$$

The decay of $f_2(2240)$ into channels with nonstrange mesons makes it verisimilar the assumption about a considerable $n\bar{n}$ component.

5) The next radial excitation on the $^3P_2n\bar{n}$ trajectory ($n = 5$) is predicted at 2490 MeV.

The trajectory [f_2(1525), f_2(1755), f_2(2120), f_2(2410)]. This is the meson trajectory with dominant $s\bar{s}$-component. The states lying on this trajectory are the nonet partners of mesons from the first trajectory [$f_2(1275)$, $f_2(1580)$, $f_2(1920)$, $f_2(2240)$]. This suggests a dominance of the P-wave in these $q\bar{q}$-systems: $^3P_2q\bar{q}$.

1) $f_2(1525)$: This is the basic state, ($n = 1$), the nonet partner of $f_2(1275)$. The mixing angle of $n\bar{n}$ and $s\bar{s}$ components, which can be determined neglecting the gluonium admixture,

$$\begin{aligned} f_2(1275) &= n\bar{n}\cos\varphi_{n=1} + s\bar{s}\sin\varphi_{n=1}, \\ f_2(1525) &= -n\bar{n}\sin\varphi_{n=1} + s\bar{s}\cos\varphi_{n=1}, \end{aligned} \qquad (7)$$

may be evaluated from the value of the partial widths $\gamma\gamma$ and ratios of the decay channels $\pi\pi$, $K\bar{K}$, $\eta\eta$ within the frame of quark combinatorics (see [5], Chapter 5 and references therein). Evaluations given in [1, 10] provide us the mixing angle as follows:

$$\varphi_{n=1} = -1^\circ \pm 3^\circ. \qquad (8)$$

2) $f_2(1755)$: This state belongs to the nonet of the first radial excitation, $n = 2$, it is dominantly the P-wave $s\bar{s}$ state. The mixing angle $\varphi_{n=2}$ can be evaluated using the data on $\gamma\gamma \to K_SK_S$. Neglecting a possible admixture of the glueball component, it was found [1]:

$$\begin{aligned} f_2(1580) &= n\bar{n}\cos\varphi_{n=2} + s\bar{s}\sin\varphi_{n=2}, \\ f_2(1755) &= -n\bar{n}\sin\varphi_{n=2} + s\bar{s}\cos\varphi_{n=1}, \\ \varphi_{n=2} &= -10^\circ \,{}^{+5^\circ}_{-10^\circ}. \end{aligned} \qquad (9)$$

3) $f_2(2120)$: This resonance was observed in the $\phi\phi$ spectrum in the reaction $\pi^-p \to n\phi\phi$ [3]. At small momenta transferred to the nucleon the pion exchange dominates, so we have the transition $\pi\pi \to \phi\phi$. The $f_2(2120)$ resonance is seen in the $\phi\phi$ system in the S-wave with the spin 2 (the state S_2). According to [2], its parameters are as follows:

$$\begin{aligned} M = 2120 \pm 30 \text{ MeV}, \quad \Gamma = 290 \pm 60 \text{ MeV}, \\ W(S_2) \simeq 90\%, \end{aligned} \qquad (10)$$

where $W(S_2)$ is the probability of the S_2-wave. The previous analysis [3], that did not account for the existence of the broad f_2-state around 2000 MeV, provided one the value $M \simeq 2010$ MeV, $\Gamma \simeq 200$ MeV [3], accordingly, this resonance was denoted as $f_2(2010)$ in [9]. At the same time, there is a resonance denoted in [9] as $f_2(2150)$, which was observed in the spectra $\eta\eta$, $\eta\eta'$, $K\bar{K}$, that assumes a large $s\bar{s}$-component:

$$\begin{array}{lll} \eta\eta\ [25]: & M = 2151 \pm 16\,\mathrm{MeV}, & \Gamma = 280 \pm 70\,\mathrm{MeV}, \\ \eta\eta\ [26]: & 2130 \pm 35\,\mathrm{MeV}, & \Gamma = 130 \pm 30\,\mathrm{MeV}, \\ \eta\eta, \eta\eta'\ [27]: & 2105 \pm 10\,\mathrm{MeV}, & \Gamma = 200 \pm 25\,\mathrm{MeV}, \\ \eta\eta\ [15]: & 2104 \pm 20\,\mathrm{MeV}, & \Gamma = 203 \pm 10\,\mathrm{MeV}, \\ K\bar{K}\ [28]: & 2130 \pm 35\,\mathrm{MeV}, & \Gamma = 270 \pm 50\,\mathrm{MeV}. \end{array} \qquad (11)$$

The re-analysis [2] points definitely to the fact that the resonances denoted in [9] as $f_2(2010)$ and $f_2(2150)$ are actually the same state.

4) $f_2(2410)$: It is seen in the reaction $\pi^- p \to n\phi\phi$ [3]. According to the re-analysis [2], its parameters are as follows:

$$\begin{gathered} M = 2410 \pm 30\ \mathrm{MeV}, \quad \Gamma = 360 \pm 70\ \mathrm{MeV}, \\ W(S_2) \simeq 50\%, \quad W(D_0) \simeq 20\%, \quad W(D_2) \simeq 30\%. \end{gathered} \qquad (12)$$

If the contribution of the broad f_2-state in the region 2000 MeV is neglected, the resonance parameters move to smaller values: $M \simeq 2340\,\mathrm{MeV}$, $\Gamma \simeq 320\,\mathrm{MeV}$ [3]; correspondingly, in [9] it was denoted as $f_2(2340)$.

5) The linearity of the (n, M^2) trajectory predicts the next ${}^3P_2 s\bar{s}$ state at 2630 MeV ($n = 5$).

The states with dominant ${}^3F_2 n\bar{n}$ component. At the time being we may speak about the observation of the two states with the dominant ${}^3F_2 n\bar{n}$-component.

1) $f_2(2020)$: It is seen in the partial wave analysis of the reactions $p\bar{p} \to \pi^0\pi^0, \eta\eta, \eta\eta'$, in the wave ${}^3F_2 p\bar{p}$ [8]. According to [6, 18], its parameters are as follows:

$$M = 2020 \pm 30\ \mathrm{MeV}, \quad \Gamma = 275 \pm 35\ \mathrm{MeV}. \qquad (13)$$

In [9], this meson was placed to the Section "Other light mesons", it is denoted as $f_2(2000)$. This is the basic ${}^3F_2$-meson ($n = 1$) with the dominant $n\bar{n}$-component.

2) $f_2(2300)$: It is seen in the partial wave analysis of the reaction $p\bar{p} \to \pi^0\pi^0, \eta\eta, \eta\eta'$, in the wave ${}^3F_2 p\bar{p}$ [8]. According to [6, 18], its parameters are as follows:

$$M = 2300 \pm 35\ \mathrm{MeV}, \quad \Gamma = 290 \pm 50\ \mathrm{MeV}. \qquad (14)$$

This is the first radial excitation of the ${}^3F_2$-state ($n = 2$), with dominant $n\bar{n}$-component. There is a resonance denoted in [9] as $f_2(2300)$, but this is the state observed in the $\phi\phi$-spectrum [3], the mass and width of which, in accordance with the re-analysis [2], are $2340 \pm 15\,\mathrm{MeV}$ and $150 \pm 50\,\mathrm{MeV}$ – of course, they are different states, see the discussion below.

3) The second radial excitation state ($n = 3$) on the trajectory ${}^3F_2 n\bar{n}$ is predicted to be at $M \simeq 2550\,\mathrm{MeV}$.

The state with dominant ${}^3F_2 s\bar{s}$ component. This trajectory is marked by one observed state only.

1) $f_2(2340)$: It is seen in the $\phi\phi$-spectrum [3] and $\gamma\gamma \to K^+K^-$ [29], with the mass $\sim 2330\,\mathrm{MeV}$ and width 275 ± 60 MeV. According to [2],

$$\begin{gathered} M = 2340 \pm 15\ \mathrm{MeV}, \quad \Gamma = 150 \pm 50\ \mathrm{MeV}, \\ W(S_2) \simeq 10\%, \quad W(D_0) \simeq 10\%, \quad W(D_2) \simeq 80\%. \end{gathered} \qquad (15)$$

In the previous analysis of the $\phi\phi$-spectrum [3], this resonance had the mass 2300 MeV, in [9] it is denoted as $f_2(2300)$.

2) The next state on the ${}^3F_2 s\bar{s}$ trajectory ($n = 2$) should be located near $M \simeq 2575\,\mathrm{MeV}$.

The broad 2^{++}-state near 2000 MeV – the tensor glueball. The averaging over parameters of the broad resonance using the data [2, 7, 8], see (1), gives us the following values:

$$M = 2000 \pm 30\ \mathrm{MeV}, \quad \Gamma = 530 \pm 40\ \mathrm{MeV}. \qquad (16)$$

This broad state is superfluous with respect to $q\bar{q}$-trajectories on the (n, M^2)-plane, i.e. it is the exotics. It is reasonable to believe that this is the lowest tensor glueball. This statement is favoured by the estimates of parameters of the pomeron trajectory (e.g. see [5], Chapter 5.4, and references therein), according to which $M_{2^{++}\mathrm{glueball}} \simeq 1.7 - 2.5\,\mathrm{GeV}$. Lattice calculations result in a close value, namely, $2.2 - 2.4\,\mathrm{GeV}$ [30].

Another characteristic signature of the glueball is its large width, that was specially underlined in [31]. The matter is that exotic state accumulates the widths of its neighbours–resonances due to the transitions $meson(1) \to real\,mesons \to meson(2)$.

Just this phenomenon took place with the lightest scalar glueball near 1500 MeV: the decay processes led to a strong mixing of the glueball with neighbouring resonances, so the glueball turned into the broad resonance $f_0(1200 - 1600)$ [32–35], see also the discussion in [6]. Of course, the width of this scalar isoscalar state is rather large, though its precise value is poorly determined: $\Gamma \simeq 500-1500\,\mathrm{MeV}$. Although the accuracy in the determination of absulute value is low, the ratios of partial widths of this state to channels $\pi\pi, K\bar{K}, \eta\eta, \eta\eta'$ are well defined [36]. So the ratios $\Gamma(\pi\pi) : \Gamma(K\bar{K}) : \Gamma(\eta\eta) : \Gamma(\eta\eta')$ tell us definitely that $f_0(1200-1600)$ is a mixture of the gluonium (gg) and quarkonium ($q\bar{q}$) components being close to the flavour singlet $(q\bar{q})_{\mathrm{glueball}}$. Namely,

$$\begin{gathered} gg \cos\gamma + (q\bar{q})_{\mathrm{glueball}} \sin\gamma, \\ (q\bar{q})_{\mathrm{glueball}} = n\bar{n} \cos\varphi_{\mathrm{glueball}} + s\bar{s} \sin\varphi_{\mathrm{glueball}} \end{gathered} \qquad (17)$$

Channel	Constants for glueball decays in the leading order of $1/N$ expansion	Constants for glueball decays in next-to-leading order of $1/N$ expansion	Identity factor for decay products
$\pi^0\pi^0$	G^L_P	0	1/2
$\pi^+\pi^-$	G^L_P	0	1
K^+K^-	$\sqrt{\lambda}\,G^L_P$	0	1
$K^0\bar{K}^0$	$\sqrt{\lambda}\,G^L_P$	0	1
$\eta\eta$	$G^L_P(\cos^2\theta+\lambda\sin^2\theta)$	$2G^{NL}_P\left(\cos^2\theta-\sqrt{\frac{\lambda}{2}}\sin^2\theta\right)^2$	1/2
$\eta\eta'$	$G^L_P(1-\lambda)\sin\theta\cos\theta$	$2G^{NL}_P\left(\cos\theta-\sqrt{\frac{\lambda}{2}}\sin\theta\right)\times\left(\sin\theta+\sqrt{\frac{\lambda}{2}}\cos\theta\right)$	1
$\eta'\eta'$	$G^L_P(\sin^2\theta+\lambda\cos^2\theta)$	$2G^{NL}_P\left(\sin\theta+\sqrt{\frac{\lambda}{2}}\cos\theta\right)^2$	1/2
$\rho^0\rho^0$	G^L_V	0	1/2
$\rho^+\rho^-$	G^L_V	0	1
$K^{*+}K^{*-}$	$\sqrt{\lambda}\,G^L_V$	0	1
$K^{*0}\bar{K}^{*0}$	$\sqrt{\lambda}\,G^L_V$	0	1
$\omega\omega$	G^L_V	$2G^{NL}_V$	1/2
$\omega\phi$	$G^L_V(1-\lambda)\varphi_V$	$2G^{NL}_V\left(\sqrt{\frac{\lambda}{2}}+\varphi_V\left(1-\frac{\lambda}{2}\right)\right)$	1
$\phi\phi$	$\lambda\,G^L_V$	$2G^{NL}_V\left(\frac{\lambda}{2}+\sqrt{2\lambda}\,\varphi_V\right)$	1/2

The constants of the tensor glueball decay into two mesons in the leading (planar diagrams) and next-to-leading (non-planar diagrams) terms of $1/N$-expansion. Mixing angles for $\eta-\eta'$ and $\omega-\phi$ mesons are defined as follows: $\eta=n\bar{n}\cos\theta-s\bar{s}\sin\theta$, $\eta'=n\bar{n}\sin\theta+s\bar{s}\cos\theta$ and $\omega=n\bar{n}\cos\varphi_V-s\bar{s}\sin\varphi_V$, $\phi=n\bar{n}\sin\varphi_V+s\bar{s}\cos\varphi_V$. Because of the small value of φ_V, we keep in the Table the terms of the order of φ_V only

with $\varphi_{\rm glueball}=\arctan\sqrt{\lambda/2}\simeq 26^\circ-33^\circ$. The mixing angle $\varphi_{\rm glueball}$ is determined by the fact that the gluon field creates the light quark pairs with probabilities $u\bar{u}:d\bar{d}:s\bar{s}=1:1:\lambda$, and the probability to produce strange quarks (λ) is suppressed $\lambda\simeq 0.5-0.8$ (see [37] and the discussion in Chapter 5 of [5]). The mixing angle γ for gluonium and quarkonium components cannot be defined by the ratios $\Gamma(\pi\pi):\Gamma(K\bar{K}):\Gamma(\eta\eta):\Gamma(\eta\eta')$ – it should be fixed by radiative transitions, for example, $\gamma\gamma\to f_0(1200-1600)$; such an experimental information is still missing. One may find a detailed discussion of the situation in [5, 6].

If the broad resonance $f_2(2000)$ is the tensor glueball, it must be also the mixture of components gg and $(q\bar{q})_{\rm glueball}$. Then the decay vertices of $f_2(2000)\to\pi\pi$, $K\bar{K}$, $\eta\eta$, $\eta\eta'$, $\eta'\eta'$ и $f_2(2000)\to\omega\omega,\rho\rho,K^*K^*,\phi\phi,\phi\omega$ should obey the constraints shown in Table.

The decays *glueball* $\to$ *two* $q\bar{q}$*-mesons* may be realized through both planar quark–gluon diagrams and non-planar ones, the contribution from non-planar diagrams being suppressed in terms of the $1/N$-expansion [38]. One may expect that in the next-to-leading order the vertices are suppressed as $G^{NL}_P/G^L_P\sim 1/10$, $G^{NL}_V/G^L_V\sim 1/10$ – in any case such a level of suppression is observed in the decay of scalar glueball $f_0(1200-1600)$ [39]. Therefore, the next-to-leading terms are important for the channel *glueball* $\to\omega\phi$ only, for other channels they may be omitted.

In the Particle Data compilation [9] there is a narrow state $f_J(2220)$, with $J^{PC}=2^{++}$ or 4^{++} and $\Gamma\simeq 23$ MeV, which is sometimes discussed as a candidate for tensor glueball, under the assumption $J=2$ (see [40] and references therein). If this state does exist with $J=2$, we see that there is no room for it on the $q\bar{q}$-trajectories shown in Fig.1: in this case it should be also considered as an exotic state.

In the mean time there exist two statements about the value of glueball width: according to [41], it should be less than hadronic widths of $q\bar{q}$-mesons, while, following [6, 31], it must be considerably greater. The arguments given in [41] are based on the evaluation of the decay couplings in lattice calculations. However, such calculations does not take into account the large-distance processes, such as *meson*$(1)\to$ *real mesons* $\to$ $\to$ *meson*(2) in case of resonance overlapping. And just these transitions are responsible for the large width of a state which is exotic by its origin [31]. The phenomenon of width accumulation for meson resonances has been studied in [32–35], but much earlier this phenomenon was observed in nuclear physics [42–44]. Therefore, I think that at present time just the large width of $f_2(2000)$ is an argument in favour of the glueball origin of this resonance. But to prove the glueball nature of $f_2(1200)$ the measurement of decay constants and their comparison to the ratios given in Table is needed.

I am grateful to L. G. Dakhno, S. S. Gershtein, V. A. Nikonov and A. V. Sarantsev for stimulating discussions, comments and help. The paper was supported by the Russian Foundation for Basic Research, project # 04-02-17091.

---

1. V. A. Schegelsky, A. V. Sarantsev, and V. A. Nikonov, L3 Note 3001 (20040).
2. R. S. Longacre and S. J. Lindenbaum, Report BNL-72371-2004.
3. A. Etkin et al., Phys. Lett. **B165**, 217 (1985); **B201**, 568 (1988).
4. A. V. Anisovich, V. V. Anisovich, and A. V. Sarantsev, Phys. Rev. **D62**, 051502 (2000).
5. V. V. Anisovich, M. N. Kobrinsky, J. Nyiri, and Yu. M. Shabelski, *Quark model and high energy collisions*, World Scientific, 2nd Edition, 2004.
6. V. V. Anisovich, UFN **174**, 49 (2004) [Physics Uspekhi **47**, 45 (2004)].
7. D. Barberis et al. (WA 102 Collab.), Phys. Lett. **B471**, 440 (2000).
8. A. V. Anisovich et al., Phys. Lett. **B491**, 47 (2000).
9. S. Eidelman et al. (PDG), Phys. Lett. **B592**, 1 (2004).
10. A. V. Anisovich, V. V. Anisovich, M. A. Matveev, and V. A. Nikonov, Yad. Fiz. **66**, 946 (2003) [Phys. Atom. Nucl. **66**, 914 (2003)].
11. A. V. Anisovich, V. V. Anisovich, and V. A. Nikonov, Eur. Phys. J. **A12**, 103 (2001).
12. E. Aker et al. (Crystall Barrel Collab.), Phys. Lett. **B260**, 249 (1991).
13. A. Adamo et al. (OBELIX Colab.), Phys. Lett. **B287**, 368 (1992); Nucl. Phys. **A558**, 13C (1993).
14. A. Bertin et al. (OBELIX Collab.), Phys. Lett. **B408**, 476 (1997).
15. T. A. Armstrong et al. (E760 Collab.), Phys. Lett. **B307**, 394 (1993); **B307**, 399 (1993).
16. V. V. Anisovich, D. S. Armstrong, I. Augustin et al. (Crystal Barrel Collab.), Phys. Lett. **B323**, 233 (1994).
17. V. V. Anisovich, D. V. Bugg, A. V. Sarantsev, and B. S. Zou, Phys. Rev. **D50**, 1972 (1994).
18. A. V. Anisovich, V. A. Nikonov, A. V. Sarantsev, and V. V. Sarantsev, in *PNPI XXX, Scientific Highlight, Theoretical Physics Division*, Gatchina, 2001, p. 58.
19. D. V. Bugg et al., Phys. Lett. **B353**, 378 (1995).
20. G. M. Beladidze et al. (VES Collab.), Z. Phys. **C54**, 367 (1992).
21. D. M. Alde et al. (GAMS Collab.), Phys. Lett. **B241**, 600 (1990).
22. D. Barberis et al. (WA 102 Collab.), Phys. Lett. **B484**, 198 (2000).
23. D. M. Alde et al. (GAMS Collab.), Phys. Lett. **B276**, 375 (1992).
24. D. Barberis et al. (WA 102 Collab.), Phys. Lett. **B471**, 429 (2000).
25. D. Barberis et al. (WA 102 Collab.), Phys. Lett. **A479**, 59 (2000).
26. A. V. Singovsky, Nuovo Cim. **A107**, 1911 (1994).
27. A. V. Anisovich et al., Phys. Lett. **B468**, 309 (1999).
28. D. Barberis et al. (WA 102 Collab.), Phys. Lett. **B453**, 305 (1999).
29. K. Abe et al. (BELLE Collab.), Eur. Phys. J. **C32**, 323 (2004).
30. G. S. Bali, K. Schilling, A. Hulsebos et al. (UK QCD Collab.), Phys. Lett. **B309**, 378 (1993); C. J. Morningstar and M. J. Peardun, Phys. Rev. **D60**, 034509 (1999).
31. V. V. Anisovich, D. V. Bugg, and A. V. Sarantsev, Phys. Rev. **D58**, 111503 (1998).
32. V. V. Anisovich, Yu. D. Prokoshkin, and A. V. Sarantsev, Phys. Lett. **B389**, 388 (1996).
33. V. V. Anisovich, Yu. D. Prokoshkin, and A. V. Sarantsev, Z. Phys. **A357**, 123 (1997).
34. A. V. Anisovich, V. V. Anisovich, and A. V. Sarantsev, Phys. Lett. **B395**, 123 (1997).
35. A. V. Anisovich, V. V. Anisovich, and A. V. Sarantsev, Z. Phys. **A359**, 173 (1997).
36. V. V. Anisovich and A. V. Sarantsev, Eur. Phys. J. **A16**, 229 (2003).
37. K. Peters and E. Klempt, Phys. Lett. **B352**, 467 (1995).
38. G. t'Hooft, Nucl. Phys. **B72**, 461 (1974); G. Veneziano, Nucl. Phys. **B117**, 519 (1976).
39. V. V. Anisovich, A. A. Kondashov, Yu. D. Prokoshkin et al., Yad. Fiz. **63**, 1489 (2000) [Phys. Atom. Nucl. **63**, 1410 (2000)].
40. M. Doser, Phys. Lett. **B592**, 594 (2004).
41. J. Sexton, A. Vaccarino, and D. Weingarten, Phys. Rev. Lett. **75**, 4563 (1995); W. Lee, D. Weingarten, Phys. Rev. **D61**, 014015 (2000).
42. I. S. Shapiro, Nucl. Phys. **A122** 645 (1968).
43. I. Yu. Kobzarev, N. N. Nikolaev, and L. B. Okun, Yad. Fiz. **10**, 864 (1969); [Sov. J. Nucl. Phys. **10**, 499 (1960)].
44. L. Stodolsky, Phys. Rev. **D1**, 2683 (1970).